

BXD Mice and TAS1R2 Sweet Taste Receptor Expression: A Hypothesis Generating Study

Ian Brown, Kendall King, George A Kyriazis

1. Introduction

The use of naturally occurring human single nucleotide polymorphisms (SNPs) and laboratory-generated mouse models are two of the most common approaches when studying gene loss-of-function (LOF). Each method provides different insights into the gene(s) of interest. Human LOF induced by SNPs often causes partial functional impairment, which gives insights into gene redundancy, evolutionary adaptation, and population-level variability [1,2]. On the other hand, LOF via laboratory-generated mouse models is induced by complete gene inactivation, allowing researchers to more fully understand gene function and promotes an environment to model human disease [3,4].

Translating and interpreting results between human LOF SNP carriers and knockout mouse models is difficult because the mouse models do not fully address observations seen in human carriers. The differences between partial and complete LOF also introduces distinct phenotypic outcomes, species-specific differences in gene regulation, genomic context, and compensatory mechanisms, making comparisons more complicated [4]. Additionally, human data is observed within outbred populations, whereas mouse models are typically observed within inbred populations. These anomalies between the two methods highlight the need to integrate both genetically diverse and graded functional loss mouse models.

This need is addressed by the BXD recombinant inbred (RI) panel, derived from C57BL/6J and DBA/2J mouse strains; it is the largest and most extensively characterized genetic reference population (GRP). With ~160 isogenic strains, the BXD RI panel has a broad range of naturally occurring genetic variation and preserves experimental reproducibility [5]. More so, BXD strains – unlike traditional RI panels – exhibit increased recombination events, leading to more genetic diversity for an improved representative model of human populations [5,6].

The use of BXD mice is common in systems genetics studies of complex traits, such as, metabolism, behavior, and molecular regulation [7]. GeneNetwork.org and other public databases facilitate quantitative trait locus (QTL) mapping and genome-wide-association studies (GWAS) within this panel. Researchers are able to use these databases to identify genetic determinants of metabolic and other complex disorders [6]. Having genetic diversity similar to human populations while retaining experimental

control of traditional RI mouse models, the BXD panel enables paralleling the graded LOF effects often seen in human SNP carriers by investigating gene function across expression levels [6,8,9].

The *Tas1r2* gene encodes the G-protein-coupled receptor (GPCR) involved in taste sensing on the tongue [10] and in peripheral nutrient metabolism [11]. A number of metabolic associations [16-18] have also been observed in humans with the *TAS1R2* Ile191Val (rs35874116) polymorphism (*TAS1R2*^{Ile191Val}), resulting in partial LOF due to receptor complex membrane instability [19]. Carriers of this polymorphism are observed to have reduced glucose excursions during an oral glucose challenge [19], similarly seen in bKO mice. Further confirmation of *TAS1R2*^{Ile191Val} effects on glucose metabolism were established in two independent studies that had individuals with partial LOF displaying lower glycosylated hemoglobin (HbA1c) [20,21], an essential measure of glucose homeostasis. Whole-body studies of *Tas1r2* knockout (bKO) C57BL/6J mice have also shown significant impacts in insulin secretion [12-14] and GLP-2 induced intestinal glucose absorption [15]. Additionally, carriers have shown improved muscle mass, mitochondrial functions, and endurance following an exercise training intervention [20]. This suggests *TAS1R2*^{Ile191Val} has a role in skeletal muscle metabolism. These observations have also been seen from studies utilizing muscle-specific *Tas1r2* deletion (mKO) [22].

A previous study has demonstrated the utility of the BXD panel in bridging the gap between clonal knockout models' outcomes and human LOF SNPs for the *Tas1r2* gene within the muscle [23]. In this study, we are leveraging these methods to explore a number of other metabolically relevant tissues to *Tas1r2*. The findings here can be used as foundational logic for hypothesis generation and further research into these tissues with phenotypic data required for meaningful biological interpretations.

2. Materials and Methods

2.1 Transcriptomics

BXD transcriptomics were run for three metabolically relevant tissues to *Tas1r2*, consisting of brown adipose tissue (BAT), heart, and liver. Data was from 29-week-old male BXD mice sourced from GeneNetwork.org (EPFL/LISP BXD CD Brown Adipose Affy Mouse Gene 2.0 ST Exon Level (Oct13) RMA; EPFL/LISP BXD CD Heart Affy Mouse Gene 2.0 ST Exon Level (Jan14) RMA; EPFL/LISP BXD CD Liver Affy Mouse Gene 1.0 ST (Apr13) RMA Exon Level). Metadata is available on the summary page provided by GeneNetwork.org.

2.2 Gene Set Enrichment and Overrepresentation Analysis

Gene Set Enrichment Analysis (GSEA) was performed using GeneTrail 3.2 (<https://genetrail.bioinf.uni-sb.de/index?pipeline=gene>). Over-representation analysis (ORA) was conducted through the WEB-based Gene SeT AnaLysis Toolkit (WebGestalt 2024). Both GSEA and ORA were applied to WikiPathways to identify functionally enriched gene sets and to provide insights into the biological roles Tas1r2 has in different tissues. All data for analysis were prepared using RStudio (version 2025.05.1+513).

2.3 Statistics

Statistical analyses were performed using RStudio (version 2025.05.1+513). T-tests were conducted to compare gene expression between BXD H_{Tas1r2} and BXD L_{Tas1r2} groups. Pearson's correlation analysis identified genes significantly associated with Tas1r2 expression in the BXD datasets.

3. Results

3.1 Tas1r2 Expression Ranking and Correlation Analysis of Genetically Diverse BXD Mice

All tissues mRNA expression data were accessed from the GeneNetwork.org datasets previously mentioned in the EPFL/LISP BXD cohort. Each dataset was comprised of several probes for Tas1r2, with only one being selected for analysis (BAT Probe ID: 17420803; Heart Probe ID: 17420803; Liver Probe ID: 10509812). These probes were selected for analysis due to their lack of cross-hybridization, normal expression distribution, and broad dynamic range across mouse strains (Figure 1A-C). To explore potential regulatory networks, an unbiased correlation analysis between Tas1r2 expression and varying gene targets (BAT gene targets = 25,434; Heart gene targets = 25,440; Liver gene targets = 16,035). This revealed a wide range of significantly correlated genes (BAT = 1,106; Heart = 2,219; Liver = 888) with Tas1r2 expression ($p < 0.05$). BAT over-representation analysis (ORA; WebGestalt 2024) identified enrichment in pathways shown below (Figure 1D). Heart ORA identified enrichment in pathways shown below (Figure 1E). Liver ORA identified enrichment in pathways shown below (Figure 1F).

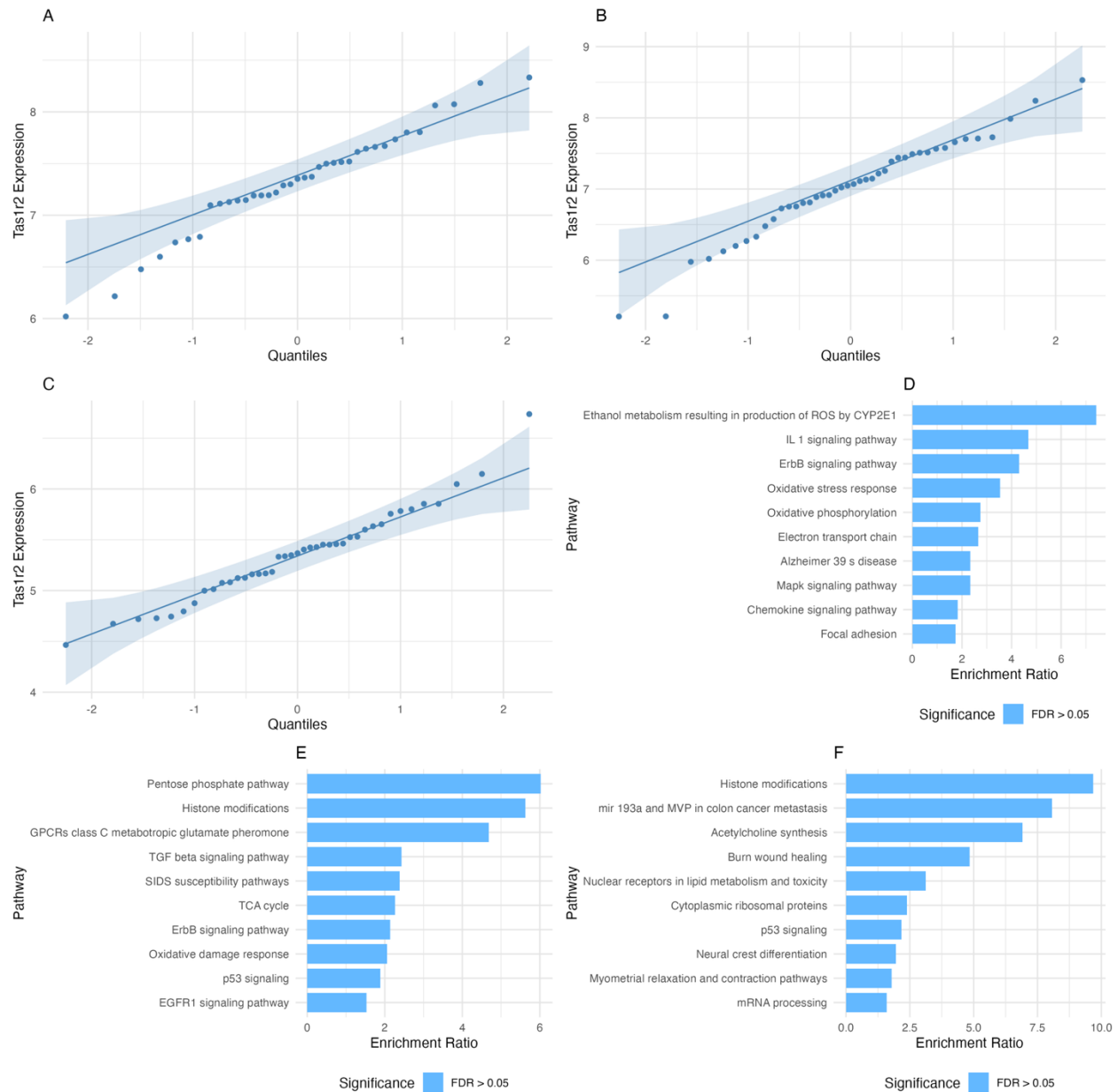


Figure 1. Tas1r2 Normal Probability and Overrepresentation Analysis (ORA) in Brown Adipose Tissue (BAT), Heart, and Liver. (A) Normal probability plot of Tas1r2 expression across BAT of BXD mice (n=37). (B) Normal probability plot of Tas1r2 expression across Heart of BXD mice (n=39). (C) Normal probability plot of Tas1r2 expression across Liver of BXD mice (n=40). (D) ORA of highly correlated genes to pathways (Wikipathways) grouped by functional categories in BAT. (E) ORA of highly correlated genes to pathways (Wikipathways) grouped by functional categories in Heart. (F) ORA of highly correlated genes to pathways (Wikipathways) grouped by functional categories in Liver.

Due to Tas1r2 forming an obligate heterodimer with Tas1r3, correlation between Tas1r2 and Tas1r3 expression were assessed. There was no significant correlation found between the two genes in any of the analyzed tissues (BAT $R = -0.11$, $p = 0.5$; Heart $R = 0.13$, $p = 0.41$; Liver $R = -0.13$, $p = 0.42$) (Figure 2A-C).

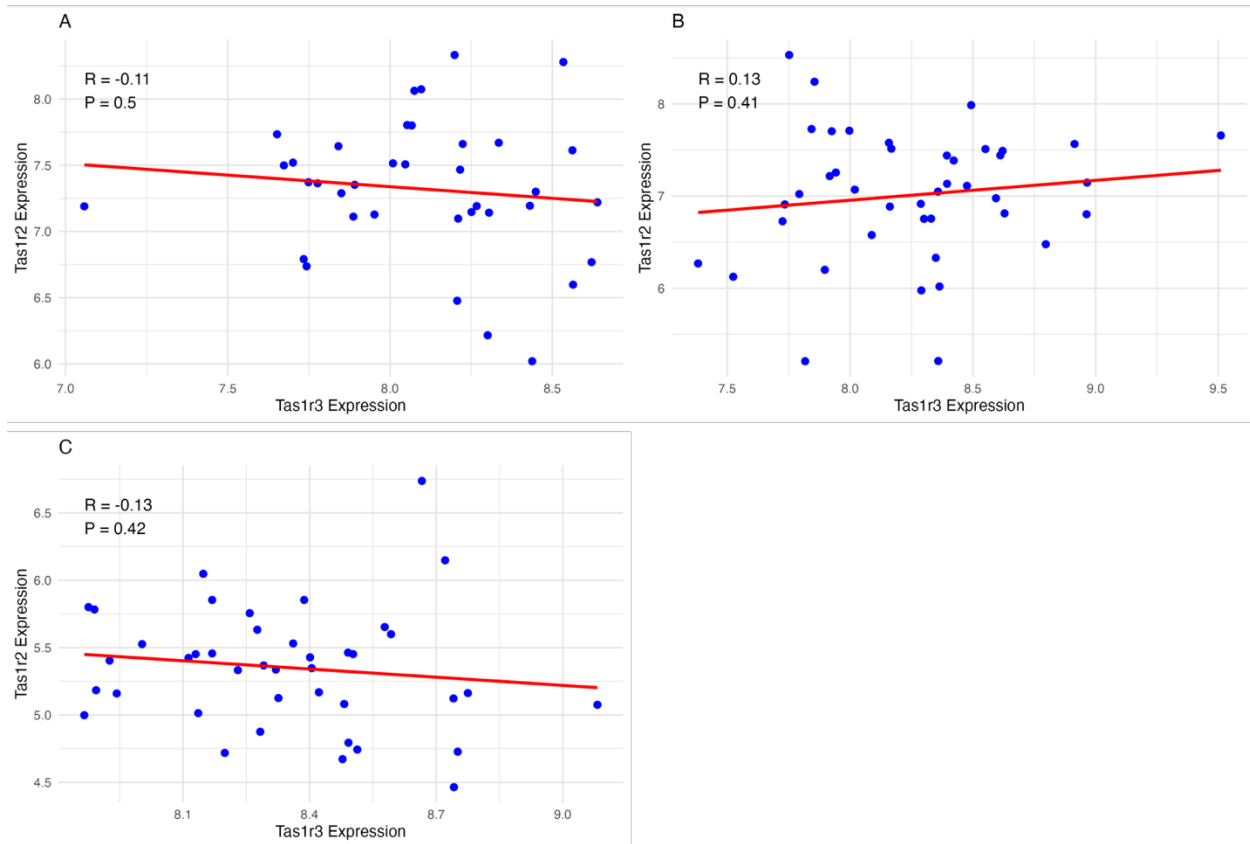


Figure 2. (A) Correlation between Tas1r2 and Tas1r3 expression in BAT of BXD mice (n=37). (B) Correlation between Tas1r2 and Tas1r3 expression in Heart of BXD mice (n=39). (C) Correlation between Tas1r2 and Tas1r3 expression in Liver of BXD mice (n=40).

3.2 Gene Set Enrichment Analysis (GSEA) of BXD Mice Stratified by Tas1r2 Expression

To investigate if variability in Tas1r2 expression leads to distinct transcriptomic signatures, Tas1r2 expression was ranked across BXD strains for each tissue (BAT = 37; Heart = 42; Liver = 40) and observed fold differences between the highest- and lowest-expression strains (BAT = 4.97; Heart = 9.99; Liver = 4.83). BXD strains were stratified into high Tas1r2 (H_{Tas1r2} , top quartile, BAT n = 10, Heart n = 11, Liver n = 11) and low Tas1r2 (L_{Tas1r2} , bottom quartile, BAT n = 10, Heart n = 11, Liver n = 11), confirming significant differences between Tas1r2 expression of the high and low groups (BAT $p = 3.1e-07$; Heart $p = 3.1e-08$; Liver $p = 6e-08$) (Figure 3A-C). Tas1r3 expression remained unchanged between groups (BAT $p = 0.66$; Heart $p = 0.22$; Liver $p = 0.27$) (Figure 3D-F), reinforcing Tas1r2 expression being responsible for transcriptomic differences rather than Tas1r3-mediated effects.

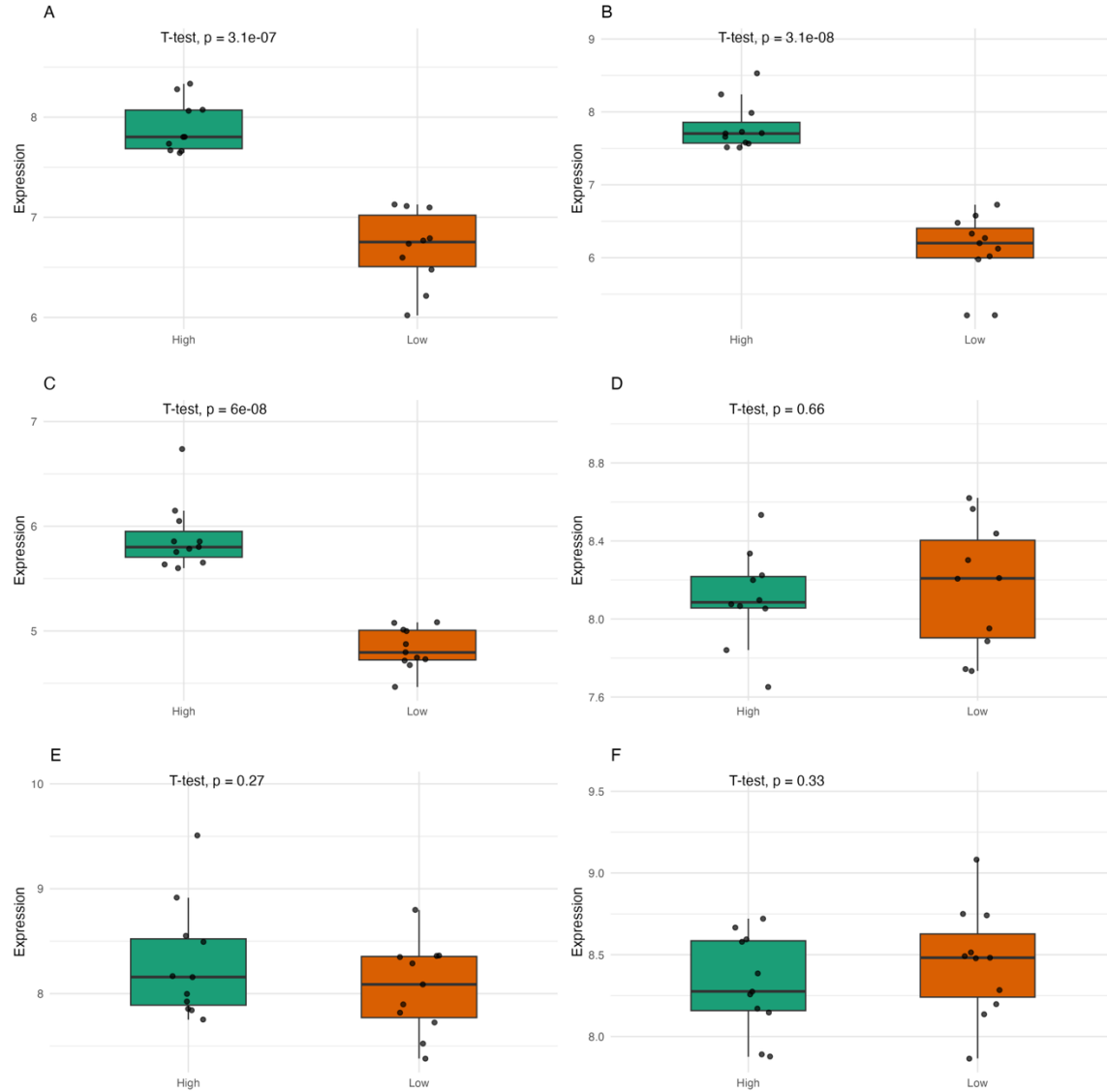


Figure 3. T-test of Tas1r2 and Tas1r3 expression stratified by Tas1r2 expression. (A) Tas1r2 expression level in H_{Tas1r2} and L_{Tas1r2} in BAT of BXD groups (H_{Tas1r2} , n=10, top quartile)(L_{Tas1r2} , n=10, bottom quartile)(p=3.1e-07). (B) T-test of Tas1r2 expression level in H_{Tas1r2} and L_{Tas1r2} in Heart of BXD groups (H_{Tas1r2} , n=11, top quartile)(L_{Tas1r2} , n=11, bottom quartile)(p=3.1e-08). (C) T-test of Tas1r2 expression level in H_{Tas1r2} and L_{Tas1r2} in Liver of BXD groups (H_{Tas1r2} , n=11, top quartile)(L_{Tas1r2} , n=11, bottom quartile)(p=6e-08). (D) T-test of Tas1r3 expression level in H_{Tas1r2} and L_{Tas1r2} in BAT of BXD groups (H_{Tas1r2} , n=10, top quartile)(L_{Tas1r2} , n=10, bottom quartile)(p=0.66). (E) T-test of Tas1r3 expression level in H_{Tas1r2} and L_{Tas1r2} in Heart of BXD groups (H_{Tas1r2} , n=11, top quartile)(L_{Tas1r2} , n=11, bottom quartile)(p=0.27). (F) T-test of Tas1r3 expression level in H_{Tas1r2} and L_{Tas1r2} in Liver of BXD groups (H_{Tas1r2} , n=11, top quartile)(L_{Tas1r2} , n=11, bottom quartile)(p=0.33).

GSEA analysis between BXD L_{Tas1r2} and BXD H_{Tas1r2} groups identified any significantly enriched pathways. BAT showed enrichment and depletion of pathways shown below (Figure 4A). Liver showed depletion of pathways shown below (Figure 4B). Remarkably, despite the extreme fold difference, heart did not show any enrichment or depletion of pathways. ORA of L_{Tas1r2} and H_{Tas1r2} were run separately to try and identify why this is (Figure 5A-B). Heatmaps of differentially expressed genes were generated to further investigate the data (Figure 6A-C).

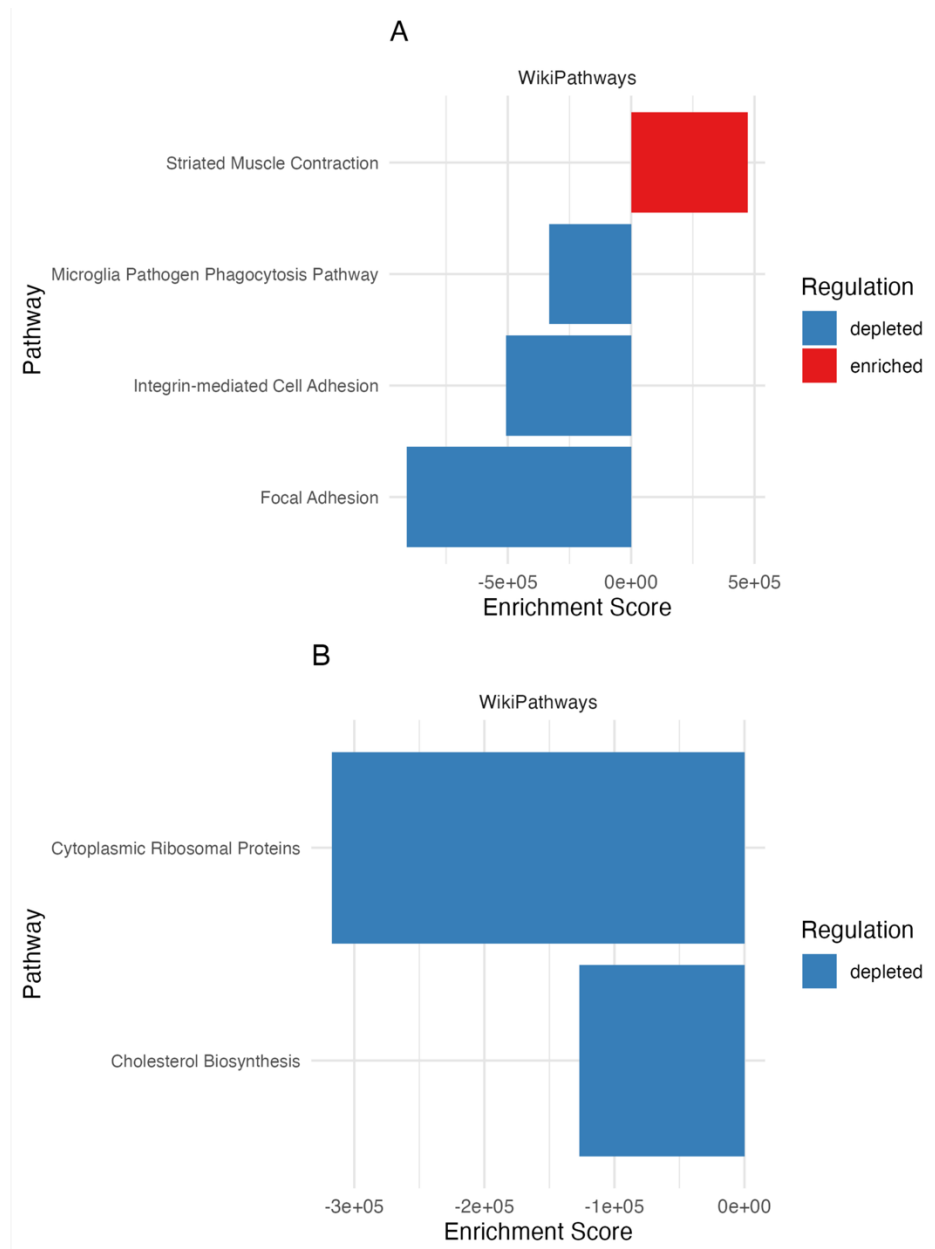


Figure 4. Gene Set Enrichment Analysis (GSEA) in BXD mice stratified by *Tas1r2* expression. (A) GSEA (Wikipathways) of BAT in BXD mice. (B) GSEA (Wikipathways) of Liver in BXD mice.

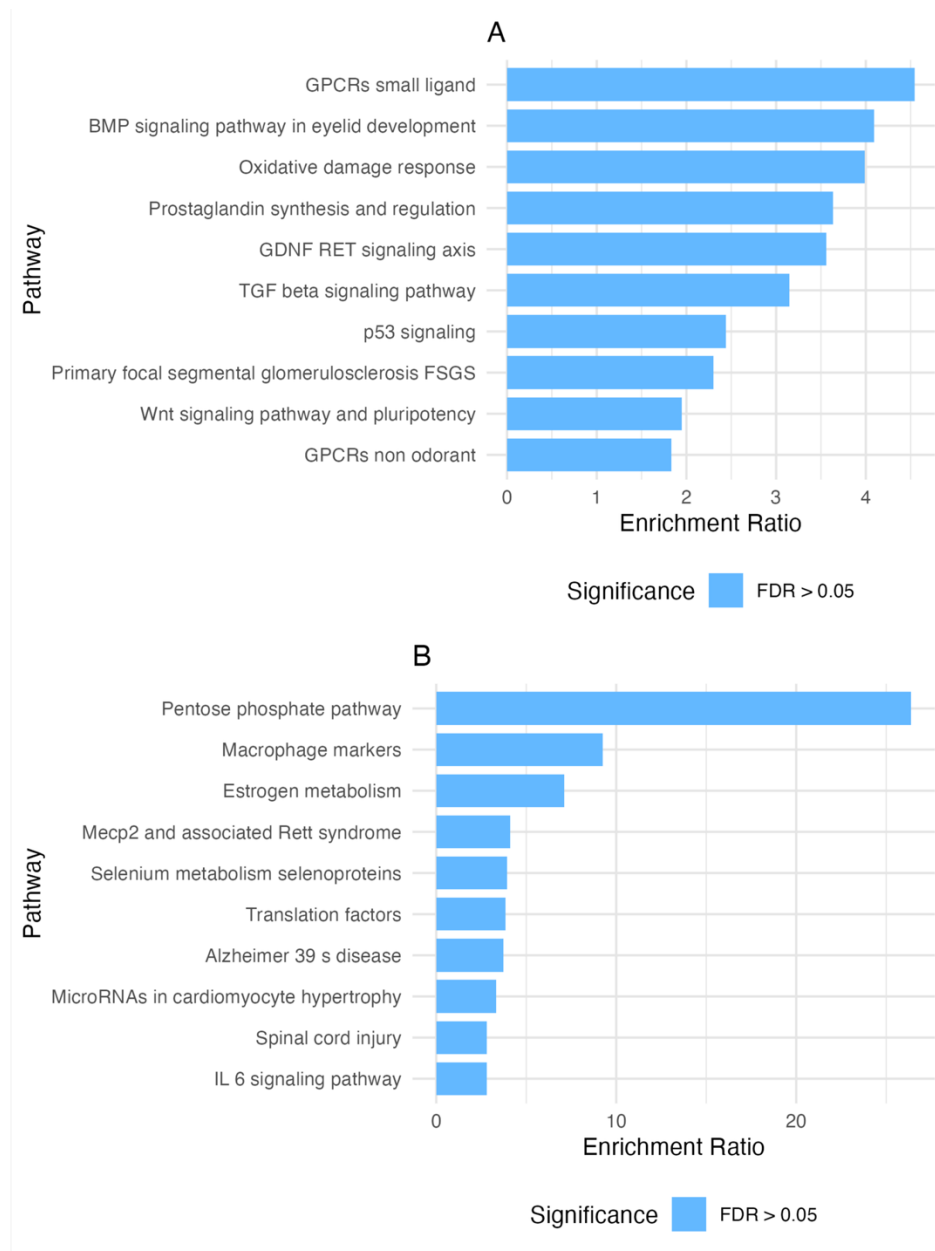


Figure 5. Overrepresentation Analysis (ORA) of stratified BXD mice in the Heart by H_{Tas1r2} and L_{Tas1r2}. (A) H_{Tas1r2} group ORA. (B) L_{Tas1r2} group ORA.

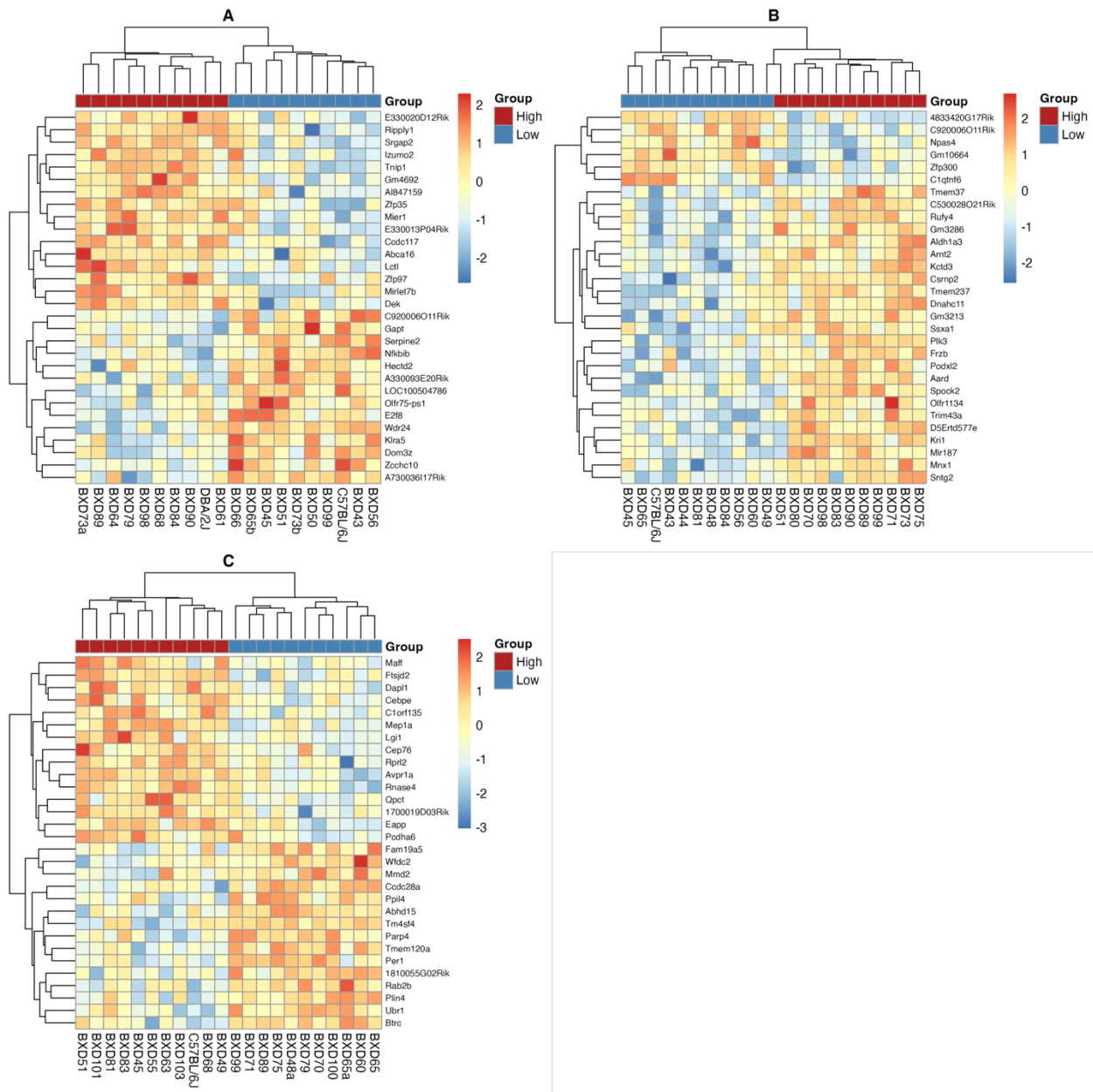


Figure 6. Heatmaps of top 30 differentially expressed genes of stratified BXD mice by H_{Tas1r2} and L_{Tas1r2} . (A) BAT heatmap. (B) Heart heatmap. (C) Liver heatmap.

4. Discussion

The ability of cells to maintain metabolic homeostasis depends on their capacity to sense and respond to nutrient availability. Specialized receptors, such as the G protein-coupled receptor $Tas1r2$, are integral to regulating downstream signaling pathways. Although the $Tas1r2$ sweet taste receptor is primarily associated with gustatory

perception, emerging evidence suggests a broader role in peripheral metabolic regulation [11]. In particular, studies have shown that Tas1r2 affects nutrient sensing in skeletal muscle [21,23], highlighting the importance of exploring its influence in other metabolically relevant tissues.

Due to the lack of accompanying phenotypic data, this study relied exclusively on publicly available genetic expression data from GeneNetwork.org. Consequently, the results are limited to exploratory analyses, and no definitive biological or clinical interpretations can be made. The primary objective of this study was therefore to identify potential transcriptomic patterns associated with Tas1r2 expression that may inform future hypothesis-driven research.

Across the three tissues analyzed, gene expression exhibited a wide dynamic range across BXD mouse strains (Figure 1A–C). However, no pathways identified through overrepresentation analysis (ORA) passed false discovery rate (FDR) correction (Figure 1D–F). The low overall correlation between Tas1r2 and other genes in each tissue (BAT: 1,106; Heart: 2,219; Liver: 888) suggests that the signal-to-noise ratio may be insufficient to detect meaningful enrichment, particularly under strict multiple testing correction.

Given that Tas1r2 functions as an obligate heterodimer with Tas1r3, it was essential to confirm that observed associations were specific to Tas1r2. Correlation analyses between Tas1r2 and Tas1r3 (Figure 2A–C) showed no significant relationship, indicating that any identified patterns likely reflect Tas1r2-specific effects. This conclusion was further supported by t-tests comparing gene expression between H_{Tas1r2} and L_{Tas1r2} expressing groups. Significant differences were found for Tas1r2 expression in all tissues (Figure 3A–C), while Tas1r3 showed no significant differential expression (Figure 3D–F), supporting the specificity of the transcriptomic patterns identified.

Gene Set Enrichment Analysis (GSEA), which assesses whether predefined gene sets are overrepresented at the extremes of a ranked gene list, revealed several limitations in this context. The enrichment score (ES) in GSEA is highly sensitive to the distribution of gene rankings. If the ranked list is relatively symmetric, the ES remains near zero, reducing the likelihood of detecting enriched pathways. This limitation may explain why no pathways were detected in the heart, despite it having the greatest dynamic expression range. Conversely, BAT showed enrichment of the striated muscle contraction pathway, which is biologically implausible.

To further investigate the potential underperformance of GSEA in the heart tissue, an ORA was performed on the two striated heart subgroups of BXD mice separately. The resulting pathways (Figure 5), though not FDR-significant, may hold biological relevance and warrant further investigation with better-powered or phenotype-linked datasets.

Given the exploratory nature of the analysis, heatmaps were used to visually inspect gene expression patterns of the top 30 differentially expressed genes in each tissue (Figure

6A–C). These visualizations help assess the coherence and separability of gene expression profiles between the H_{Tas1r2} and L_{Tas1r2} groups. However, the relatively uniform expression patterns between groups likely contributed to the lack of statistically robust findings and may reflect low effect sizes or noise inherent to the dataset.

While this study does not establish causal relationships or definitive biological insights, it highlights several potential areas for deeper investigation. The analyses identified subtle patterns of differential expression and weak pathway enrichment that, if validated with complementary phenotypic or functional data, could shed light on *Tas1r2*'s role in peripheral metabolism.

Future work should focus on integrating genotype and phenotype data to evaluate the functional relevance of *Tas1r2* expression differences. Incorporating multi-omics data and employing more sophisticated statistical models or machine learning techniques may also enhance the detection of subtle regulatory signals. Overall, this study provides a foundational, exploratory framework for investigating nutrient-sensing receptors in metabolic tissues, offering hypotheses for future targeted research.

Although this study was conducted using mouse genomic data, the use of BXD recombinant inbred (RI) strains provides translational value for public health research. The BXD RI panel captures a wide range of natural genetic variation, analogous to the diversity observed in human populations. Therefore, they are a powerful resource for hypothesis generation relevant to complex traits, including metabolic health. As stated, the *Tas1r2* gene is increasingly recognized as a modulator of systemic metabolic processes [11]. As such, understanding the transcriptional effects of *Tas1r2* expression in metabolically active tissues may offer insights into nutrient sensing, energy balance, and metabolic flexibility. These functions factor closely to chronic diseases such as obesity, type 2 diabetes, and cardiovascular disease [24]. By identifying genotype-linked expression patterns in model organisms, this research lays the groundwork for future studies that could investigate analogous pathways in human cohorts, potentially contributing to risk stratification, prevention strategies, and targeted interventions.

References

1. MacArthur, D.G.; Balasubramanian, S.; Frankish, A.; Huang, N.; Morris, J.; Walter, K.; Jostins, L.; Habegger, L.; Pickrell, J.K.; Montgomery, S.B.; et al. A systematic survey of loss-of-function variants in human protein-coding genes. *Science* 2012, 335, 823-828, doi:10.1126/science.1215040.
2. Monroe, J.G.; McKay, J.K.; Weigel, D.; Flood, P.J. The population genomics of adaptive loss of function. *Heredity (Edinb)* 2021, 126, 383-395, doi:10.1038/s41437-021-00403-2.
3. Doyle, A.; McGarry, M.P.; Lee, N.A.; Lee, J.J. The construction of transgenic and gene knockout/knockin mouse models of human disease. *Transgenic Research* 2012, 21, 327-349, doi:10.1007/s11248-011-9537-3.
4. Sareila, O.; Hagert, C.; Rantakari, P.; Poutanen, M.; Holmdahl, R. Direct Comparison of a Natural Loss-Of-Function Single Nucleotide Polymorphism with a Targeted Deletion in the *Ncf1* Gene Reveals Different Phenotypes. *PLOS ONE* 2015, 10, e0141974, doi:10.1371/journal.pone.0141974.
5. Peirce, J.L.; Lu, L.; Gu, J.; Silver, L.M.; Williams, R.W. A new set of BXD recombinant inbred lines from advanced intercross populations in mice. *BMC Genetics* 2004, 5, 7, doi:10.1186/1471-2156-5-7.
6. Ashbrook, D.G.; Arends, D.; Prins, P.; Mulligan, M.K.; Roy, S.; Williams, E.G.; Lutz, C.M.; Valenzuela, A.; Bohl, C.J.; Ingels, J.F.; et al. A platform for experimental precision medicine: The extended BXD mouse family. *Cell Syst* 2021, 12, 235-247 e239, doi:10.1016/j.cels.2020.12.002.
7. Andreux, Pénélope A.; Williams, Evan G.; Koutnikova, H.; Houtkooper, Riekelt H.; Champy, M.-F.; Henry, H.; Schoonjans, K.; Williams, Robert W.; Auwerx, J. Systems Genetics of Metabolism: The Use of the BXD Murine Reference Panel for Multiscalar Integration of Traits. *Cell* 2012, 150, 1287-1299.
8. Molenhuis, R.T.; Bruining, H.; Brandt, M.J.V.; van Soldt, P.E.; Abu-Toamih Atamni, H.J.; Burbach, J.P.H.; Iraqi, F.A.; Mott, R.F.; Kas, M.J.H. Modeling the quantitative nature of neurodevelopmental disorders using Collaborative Cross mice. *Molecular Autism* 2018, 9, 63, doi:10.1186/s13229-018-0252-2.
9. Voy, B.H. Systems Genetics: a Powerful Approach for Gene-Environment Interactions. *The Journal of Nutrition* 2011, 141, 515-519.
10. Nelson, G.; Hoon, M.A.; Chandrashekar, J.; Zhang, Y.; Ryba, N.J.; Zuker, C.S. Mammalian sweet taste receptors. *Cell* 2001, 106, 381-390.
11. Calvo, S.S.; Egan, J.M. The endocrinology of taste receptors. *Nat Rev Endocrinol* 2015, 11, 213-227, doi:10.1038/nrendo.2015.7.

12. Kyriazis, G.A.; Smith, K.R.; Tyrberg, B.; Hussain, T.; Pratley, R.E. Sweet taste receptors regulate basal insulin secretion and contribute to compensatory insulin hypersecretion during the development of diabetes in male mice. *Endocrinology* 2014, 155, 2112-2121, doi:10.1210/en.2013-2015.
13. Kyriazis, G.A.; Soundarapandian, M.M.; Tyrberg, B. Sweet taste receptor signaling in beta cells mediates fructose-induced potentiation of glucose-stimulated insulin secretion. *Proc.Natl.Acad.Sci.U.S.A* 2012, 109, E524-E532, doi:1115183109 [pii];10.1073/pnas.1115183109 [doi].
14. Serrano, J.; Meshram, N.N.; Soundarapandian, M.M.; Smith, K.R.; Mason, C.; Brown, I.S.; Tyrberg, B.; Kyriazis, G.A. Saccharin Stimulates Insulin Secretion Dependent on Sweet Taste Receptor-Induced Activation of PLC Signaling Axis. *Biomedicines* 2022, 10, doi:10.3390/biomedicines10010120.
15. Smith, K.; Karimian Azari, E.; LaMoia, T.E.; Hussain, T.; Vargova, V.; Karolyi, K.; Veldhuis, P.P.; Arnoletti, J.P.; de la Fuente, S.G.; Pratley, R.E.; et al. T1R2 receptor-mediated glucose sensing in the upper intestine potentiates glucose absorption through activation of local regulatory pathways. *Mol Metab* 2018, 17, 98-111, doi:10.1016/j.molmet.2018.08.009.
16. Eny, K.M.; Wolever, T.M.; Corey, P.N.; El-Sohemy, A. Genetic variation in TAS1R2 (Ile191Val) is associated with consumption of sugars in overweight and obese individuals in 2 distinct populations. *Am J Clin Nutr* 2010, 92, 1501-1510, doi:10.3945/ajcn.2010.29836.
17. Melo, S.V.; Agnes, G.; Vitolo, M.R.; Mattevi, V.S.; Campagnolo, P.D.B.; Almeida, S. Evaluation of the association between the TAS1R2 and TAS1R3 variants and food intake and nutritional status in children. *Genet Mol Biol* 2017, 40, 415-420, doi:10.1590/1678-4685-GMB-2016-0205.
18. Ramos-Lopez, O.; Panduro, A.; Martinez-Lopez, E.; Roman, S. Sweet Taste Receptor TAS1R2 Polymorphism (Val191Val) Is Associated with a Higher Carbohydrate Intake and Hypertriglyceridemia among the Population of West Mexico. *Nutrients* 2016, 8, 101, doi:10.3390/nu8020101.
19. Serrano, J.; Seflova, J.; Park, J.; Pribadi, M.; Sanematsu, K.; Shigemura, N.; Serna, V.; Yi, F.; Mari, A.; Procko, E.; et al. The Ile191Val is a partial loss-of-function variant of the TAS1R2 sweet-taste receptor and is associated with reduced glucose excursions in humans. *Mol Metab* 2021, 54, 101339, doi:10.1016/j.molmet.2021.101339.
20. Serrano, J.; Kondo, S.; Link, G.M.; Brown, I.S.; Pratley, R.E.; Baskin, K.K.; Goodpaster, B.H.; Coen, P.M.; Kyriazis, G.A. A partial loss-of-function variant (Ile191Val) of the TAS1R2 glucose receptor is associated with enhanced responses to exercise training in older adults with obesity: A translational study. *Metabolism* 2024, 156045, doi:10.1016/j.metabol.2024.156045.

21. Serrano, J.; Yi, F.; Smith, J.; Pratley, R.E.; Kyriazis, G.A. The Ile191Val Variant of the TAS1R2 Subunit of Sweet Taste Receptors Is Associated With Reduced HbA1c in a Human Cohort With Variable Levels of Glucose Homeostasis. *Front Nutr* 2022, 9, 896205, doi:10.3389/fnut.2022.896205.
22. Serrano, J.; Boyd, J.; Brown, I.S.; Mason, C.; Smith, K.R.; Karolyi, K.; Maurya, S.K.; Meshram, N.N.; Serna, V.; Link, G.M.; et al. The TAS1R2 G-protein-coupled receptor is an ambient glucose sensor in skeletal muscle that regulates NAD homeostasis and mitochondrial capacity. *Nat Commun* 2024, 15, 4915, doi:10.1038/s41467-024-49100-8.
23. King, K., Serrano, J., Meshram, N. N., Saadi, M., Moreira, L., Papachristou, E. G., & Kyriazis, G. A. (2025). Low TAS1R2 sweet taste receptor expression in skeletal muscle of genetically diverse bxd mice mirrors transcriptomic signatures of loss-of-function mice. *Nutrients*, 17(11), 1918. <https://doi.org/10.3390/nu17111918>.
24. Chaudhari, N., & Roper, S. D. (2010). The cell biology of taste. *Journal of Cell Biology*, 190(3), 285–296. <https://doi.org/10.1083/jcb.201003144>